



Citation for published version:

Ciampa, F, Scarselli, G & Meo, M 2015, 'Nonlinear imaging method using second order phase symmetry analysis and inverse filtering', *Journal of Nondestructive Evaluation*, vol. 34, no. 2, 7, pp. 1-6.
<https://doi.org/10.1007/s10921-015-0279-7>

DOI:

[10.1007/s10921-015-0279-7](https://doi.org/10.1007/s10921-015-0279-7)

Publication date:

2015

Document Version

Peer reviewed version

[Link to publication](#)

This is a post-peer-review, pre-copyedit version of an article published in *Journal of Nondestructive Evaluation*. The final authenticated version is available online at: <https://doi.org/10.1007/s10921-015-0279-7>.

University of Bath

Alternative formats

If you require this document in an alternative format, please contact:
openaccess@bath.ac.uk

General rights

Copyright and moral rights for the publications made accessible in the public portal are retained by the authors and/or other copyright owners and it is a condition of accessing publications that users recognise and abide by the legal requirements associated with these rights.

Take down policy

If you believe that this document breaches copyright please contact us providing details, and we will remove access to the work immediately and investigate your claim.

Abstract Page

Title

Nonlinear imaging method using second order phase symmetry analysis and inverse filtering

Authors

Francesco Ciampa and Michele Meo

Material Research Centre, Department of Mechanical Engineering, University of Bath, Bath, BA2 7AY, UK

Abstract

This paper presents a nonlinear imaging method based on nonlinear elastic guided waves, for the damage detection and localisation in a composite laminate. The proposed technique relies on the study of the structural nonlinear responses by means of a combination of second order phase symmetry analysis with chirp excitation and inverse filtering method. Phase symmetry analysis was used to exploit the invariant properties of the propagating elastic waves with the phase angle of the pulse compressed chirp signals, in order to characterise the second order nonlinear behaviour of the medium. Then, the inverse filtering approach was applied to a library of second order nonlinear responses to obtain a two-dimensional image of the damage. The experimental tests carried out on an impact damage composite sample were compared to standard C-scan. The results showed that the present technique allowed achieving the optimal focalisation of the nonlinear source in the spatial and time domain, by taking advantage of multiple scattering and a small number of receiver sensors.

I. INTRODUCTION

Developments in carbon fibres reinforced plastic materials have allowed a radical advancement in lightweight aerospace applications. However, these components are sensitive to low velocity impact damage that can considerably degrade the structural integrity and, if not detected, it might result in catastrophic failures [1], [2]. Over the last few decades, innovative ultrasonic guided waves (GW) inspection methods, based on the analysis of material nonlinear elastic effects, were developed for the detection and localisation of structural defects such as micro-cracks, delaminations, weak adhesive bonds, etc... [3], [4]. Among them, nonlinear elastic wave spectroscopy (NEWS) [5], [6] [7], [8], and phase symmetry analysis (PSA) techniques [9], [10] were used to explicitly interrogate the nonlinear behaviour of the medium and its effect on the wave propagation. Indeed, by using either mono- or bi-harmonic excitation, sum and difference frequencies in addition to higher harmonics and sub-harmonics of the fundamental frequencies can be generated. Particularly, in damaged media such as aluminium, steel, composite laminates and numerous others, the nonlinear interaction of elastic waves with the structural defect can be treated as an expansion of the elastic energy as a power series with respect to the strain [11]. As a result, the contribution of the second order nonlinear effect in the acquired spectrum becomes dominant with respect to other harmonics, as the second harmonic amplitude is quadratic with the fundamental one. In addition, both experimental and numerical evidence [12], [13], [14], [15], [16], [17], showed that such a nonlinear effect can be due to the clapping contacts of the internal interfaces of a micro-crack or delamination [18], [19]. Hence, the second order nonlinear harmonic can be used to univocally indicate the presence of structural defects within the material.

In the last few years, NEWS and PSA methods were combined with time reversal acoustic (TRA) technique in order to perform a nonlinear imaging method (NIM) capable of identifying and localising the structural damage [10], [20], [21]. Indeed, due to the time invariance and spatial reciprocity of the wave equation, in a TRA experiment an input signal either from a primary source (impact point) or a secondary one (linear/nonlinear scatterer) can be focused back to the original excitation point [22], [23], [24], [25]. TRA process is usually divided into two steps, i.e. a forward and a backward propagation step. In the former step, the elastic waves diverging from the source are recorded by a set of surface bonded piezoelectric transducers. In the backward step, the acquired output is reversed in the time domain and re-emitted back onto the excitation point by using the benefit of a diffuse wave field (known as kaleidoscopic effect) [26]. However, even though spatial reciprocity and TRA invariance hold in diffuse wave fields or anisotropic media, nonlinear attenuation with the wave amplitude may induce distortions of the elastic wave front propagating into the structure. These effects may break the time reversal symmetry making the re-focusing process difficult to be interpreted [27], [28]. However, recent literature [29] showed that the inverse filtering (IF) method associated with PSA analysis allowed the recovery of the optimal refocusing at the defect location, even in dissipative media. As an example, Ciampa and Meo [10] illustrated the capability of IF and third order PSA to retrieve the damage position on a damaged composite sandwich panel showing hysteretic behaviour.

This paper presents a NIM aimed at detecting and localising the second order nonlinearity into a damaged carbon fibre reinforced plastic (CFRP) laminate using only two sensors in pitch-catch mode. The proposed technique relies on a combination of IF and second order PSA with chirp excitation, in order to obtain the optimal refocusing at the nonlinear

scatterer location due to the presence of delamination. The efficiency of this methodology is experimentally demonstrated on a composite panel undergone to impact loading, confirming that the damage location can be retrieved with high level of accuracy. Section II describes the principles of the proposed nonlinear imaging method whilst Section III reports the experimental set-up. Section IV illustrates the imaging results of the damage location on a damaged composite laminate. Then, the conclusions of this research work are presented.

II. PRINCIPLES OF THE NONLINEAR IMAGING METHOD

This Section introduces the basic concept of the nonlinear inverse filtering process along with the phase symmetry analysis used to extract the second order harmonic content in the acquired signals. Particularly, PSA was employed to characterize the nonlinear response of a damaged anisotropic medium by exploiting its symmetrical properties the phase angle ϕ of the chirp excitation signals. In other words, this method allows determining the phase angle of the input waveforms in order to discern only the nonlinear second harmonic component of the received output. The nonlinear imaging method can be defined as follows. In the *forward propagation step*, an impact loading was applied to the back surface of a CFRP composite laminate in order to generate delamination localised at the impact site, invisible from the top surface. Then the damaged zone surrounding the impact point (known as “focusing area”) was divided in $M = 8 \times 5$ “excitation points” distributed along a grid at interval of 1 cm [Fig. (1)].

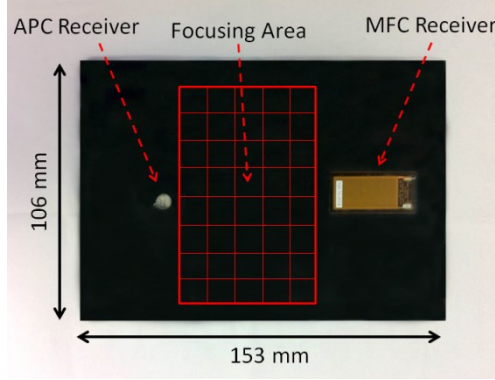


Figure 1 Representation of the composite structure. The size of each cell of the grid is 1 by 1 cm.

In each of the m ($1 \leq m \leq M$) excitation points a longer duration linear chirp signal $x(t)$ with a broad frequency band, B , ranging between 90 and 160 kHz and duration, T , of 1 ms was transmitted [Fig. (2)]. Since the time-bandwidth product TB is sufficiently large ($TB > 15$), the signal's spectrum in figure (2b) is assumed to be approximately a rectangular distribution. Then, a weighted matched filter (mismatched filter) was performed as it allows converting the transmitted signal into a band-limited pulse of greater peak power.

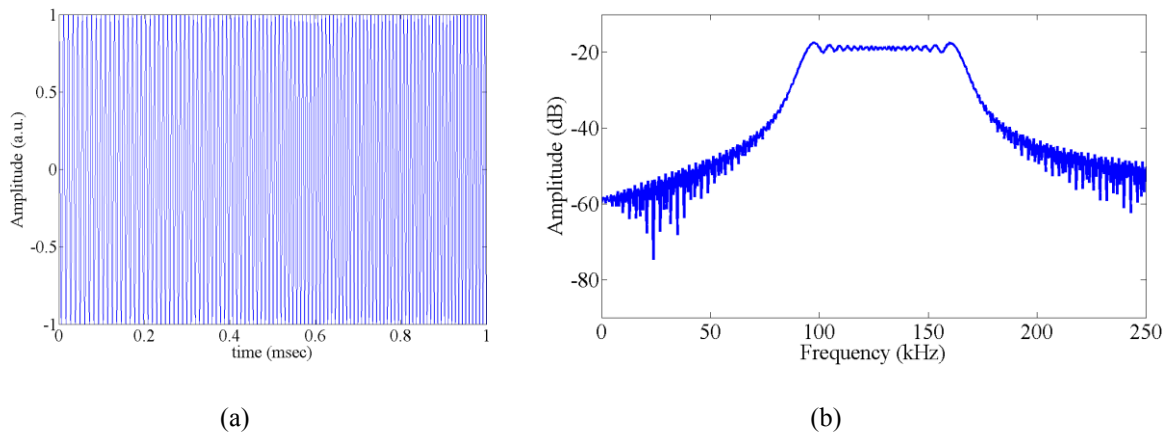


Figure 2 Signal emitted (a) and its spectrum (b).

Indeed, a mismatched filter consists of a correlation between the received and the transmitted chirp signals, and it can be expressed by the following equation [30]:

$$e(t) = \mathfrak{F}^{-1}[X(f) \cdot H_{MF}(f)] = e^{j\phi} \int_{-\infty}^{\infty} C(f) \cdot H_{MF}(f) e^{j2\pi f t} df \cong \delta(t) e^{j\phi} \quad (1)$$

wherein $e(t)$ is the new input signal to be time reversed from each excitation point, $\delta(t)$ is a temporal delta function distribution, $C(\omega)$ is the Fourier transform of the transmitted chirp waveform with null phase angle ϕ , $H_{MF}(\omega) = W(\omega)C^*(\omega)$, where $W(\omega)$ is the Fourier transform of the window function (Blackman), and the star symbol “*” corresponds to complex conjugate operation. The window function was used to shape the transmitted pulse envelope in order to reduce the resulting *sinc* side-lobes [31].

Assuming the excitation signal defined by Eq. (1), the nonlinear behaviour of the medium can be described through a nonlinear system, and the output $f(t)$ received by the sensor placed in the far field of the focusing area can be expressed through a Volterra functional series as follows [10], [32]:

$$f(t) = \mathbf{h}_m^{(1)}(t)e^{j\phi} + \beta \mathbf{h}_m^{(2)}(t)e^{j2\phi} + \gamma \mathbf{h}_m^{(3)}(t)e^{j3\phi} \quad (2)$$

where β and γ are the 2nd and 3rd order nonlinear coefficients, and the n th order kernel of Eq. (2), $\mathbf{h}_m^{(n)}(t)$, with $n = 1, 2, 3$, is called the *nonlinear impulse response* of order n . This last term includes all the nonlinear propagation effects through the medium as well as the linear contribution of the elastic waves from the m th excitation point to the receiver. Fig. 3 illustrates the output recorded by the receiver from one of the m th excitation points in the time domain and its spectrum containing the second harmonic due to the presence of a structural damage.

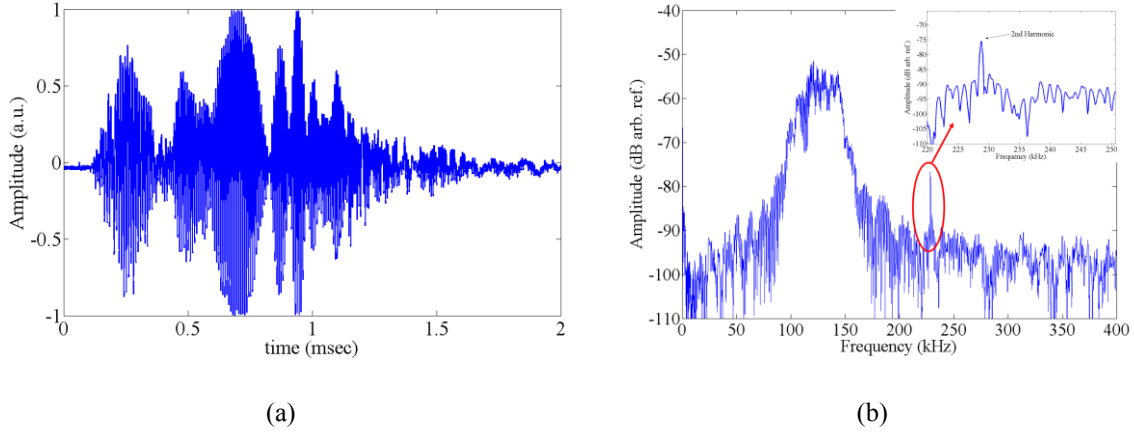


Figure 3 Acquired signal from one of the excitation points (a) and its spectrum containing the peak of the second harmonic (b).

Therefore, second order PSA can be used to eliminate both the linear and the third order nonlinear harmonic part from the signal acquired by the receiver transducer, by simply imposing the *second order symmetry condition*, $2j\phi = \pm 2\pi kj$, with $k \in \mathbb{N}$, where \mathbb{N} is the set of all natural numbers. Such invariant condition is fulfilled for two different phase angles, $\phi=0$ and $\phi=\pi$. Indeed, PSA consists in sending two phase shifted chirp waveforms into the damaged structure, in order to extract only the nonlinear second order signature:

$$f_0(t)|_{\phi=0} = \mathbf{h}_m^{(1)}(t) + \beta \mathbf{h}_m^{(2)}(t) + \gamma \mathbf{h}_m^{(3)}(t) \quad (3a)$$

$$f_\pi(t)|_{\phi=\pi} = -\mathbf{h}_m^{(1)}(t) + \beta \mathbf{h}_m^{(2)}(t) - \gamma \mathbf{h}_m^{(3)}(t) \quad (3b)$$

Hence, by simply adding the two output signals in Eqs. (3a) and (3b), yields:

$$f_{PSA}(t) = \frac{f_0(t) + f_\pi(t)}{2} = \beta \mathbf{h}_m^{(2)}(t) \quad (4)$$

where $\mathbf{h}_m^{(2)}(t)$ is the *second order nonlinear impulse response*. Figure (4) depicts the extraction of second order nonlinear signature from the sum of the structural responses originated by the input chirp signals with different phase angles.

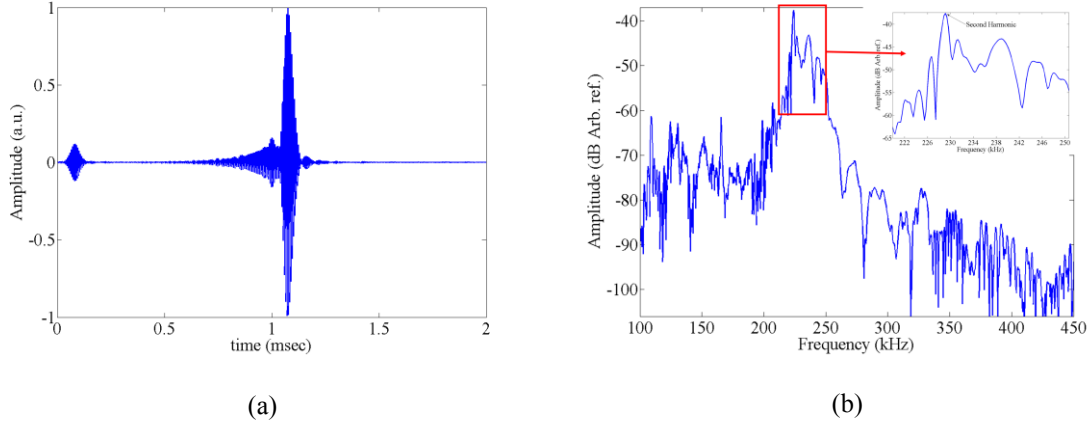


Figure 4 Signal filtered using PSA (a) and its spectrum (b). From figure (b) it can be clearly seen that only the 2nd order contribution is remained in the summation signal with a wider bandwidth from about 220 to 260 kHz and a narrow peak at 228 kHz.

Thereby, the M second order nonlinear response $\mathbf{h}_m^{(2)}(t)$ from all the point of the focusing area were stored and re-broadcasted into the medium from their original source location. In the angular frequency domain the measured nonlinear response is:

$$F_{PSA}(\omega) = \beta \mathbf{H}_m^{(2)}(\omega) \mathbf{Y}_{m_0}(\omega) \quad (5)$$

where an ideal focusing pattern vector $\mathbf{Y}_{m_0}(\omega)$ of length $M \times 1$ was introduced, which corresponds to the signal originating from the damage located in m_0 . Its components are $Y_{m_0} = 1$ for $m = m_0$ and $Y_{m_0} = 0$ for $m \neq m_0$.

The *backward propagation step* consists of focusing energy not only at the location of the nonlinearity (m_0), but also to neighbouring points (M excitation points). In fact, by means of IF method, the optimal field distribution on the receiver is determined by simply inverting the *second order nonlinear transfer matrix* $\mathbf{H}_m^{(2)}(\omega)$ in the frequency domain. Such a process would give rise after propagation to the field distribution $\mathbf{Y}_{IF}(\omega)$ on the focusing area. Thereby, all the waveforms previously acquired from the same excitation

points and processed with PSA were re-broadcasted into the medium. The back propagated signal at the damage location becomes:

$$\mathbf{Y}_{IF}(\omega) = \left[\mathbf{H}_m^{(2)T}(\omega) \right]_{IF} \tilde{\mathbf{H}}_m^{(2)} \mathbf{Y}_{m0}(\omega) \quad (6)$$

where $\tilde{\mathbf{H}}_m^{(2)} = \frac{\mathbf{H}_m^{(2)*}(\omega)}{\|\mathbf{H}_m^{(2)}(\omega)\|^2}$ is the inversion of the third order nonlinear operator and

$\|\mathbf{H}_m^{(2)}(\omega)\|^2$ is the squared norm of $\mathbf{H}_m^{(2)}(\omega)$, which represents the square of the second order nonlinear system's modal energy. Such inversion increases the number of modes employed for the back-propagation at the focal point. Indeed, the modes contained in the signal are weighted by the inverse of the energy at each eigenfrequency, ω . Hence, with the IF approach even those modes with weak energy, which are poorly exploited in a simple TRA experiment, can participate to the focusing process, thus increasing the image contrast [28]. The operator $\left[\mathbf{H}_m^{(2)T}(\omega) \right]_{IF} \cdot \tilde{\mathbf{H}}_m^{(2)}$ is referred to as the second order nonlinear IF operator and Eq. (6) has a maximum at the focus point (damage location), i.e. when $m=m_0$. Therefore, the focusing on the nonlinear scattering source can be obtained through a nonlinear “virtual” IF experiment.

III. EXPERIMENTAL SET-UP

The experiments were carried out on a composite CFRP plate with dimensions 153 x 106 x 3 mm and a lay-up sequence of [0/45/90/-45]_s [Fig. (1)]. A dropped-weight impact test machine with a hemispherical tip was used for hitting the test panel at 12 J. Such an energy level was chosen in order to inflict damage in the composite laminate corresponding to barely visible impact damage (BVID). A qualitative image of the

delamination generated by the impact was obtained through the “USL SCM 12x” ultrasonic C-Scan [Fig. (5)]. As it can be seen from Fig. (5), this linear ultrasonic test showed a circular damaged area with a radius of 10 mm composed by two internal flaws (represented by a white colour area) and an “apparent” undamaged zone in the middle. Since the protrusion occurred as a result of impact loading, the ultrasonic C-scan was not able to detect the damaged area beneath this protrusion due to poor acoustic impedance.



Figure 5 Image of the defect using ultrasonic C-Scan

In order to measure the material elastic responses, two different surface bonded receiver transducers were used, i.e. a broadband APC sensor with diameter of 6.35 mm and thickness of 2.55 mm, and a MFC-P2 transducer with length of 37 mm and width of 18 mm. Both sensors were instrumented with the NI PXI-5105 8 channel digitizer/oscilloscope card, with a sampling rate of 10 MHz. To transmit the waveforms from each of the $M = 40$ excitation points, a broadband Olympus – Panametrics NDT V106 sensor with a central frequency of 2.25 MHz was used. It was linked to a preamplifier and connected to the NI PXI 5421 16-bit arbitrary waveform generator in order to transmit the chirp signals in the forward propagation step and the inverted nonlinear responses in the backward one. The total bandwidth $B = 90\text{-}160$ kHz of the

chirp waveforms was chosen to maximise the efficiency of the available transducers. Moreover, due to the long reverberation present in the signal, a $T = 2$ ms duration time window was selected. The time histories of the measured signals were stored on a computer memory.

IV. NONLINEAR IMAGING RESULTS

According to Section II, the refocusing wave field at the damage location (placed at $x = 59$ mm and $y = 53$ mm) is represented by a normalized two-dimensional map of the correlation coefficients represented by Eq. (6), and the maximum of $\mathbf{Y}_{IF}(\omega)$ is deduced from the values nearest to 1 [Fig. (6)]. In order to show the feasibility of this “virtual” imaging method, two different cases were analyzed with the receiver transducers placed in two different positions. In case 1, the APC sensor was positioned at coordinates $x_1 = 30$ mm and $y_1 = 50$ mm [Fig. (6a)], while, in case 2, the MFC sensor was located at coordinates $x_2 = 90$ mm and $y_2 = 48$ mm [Fig. (6b)].

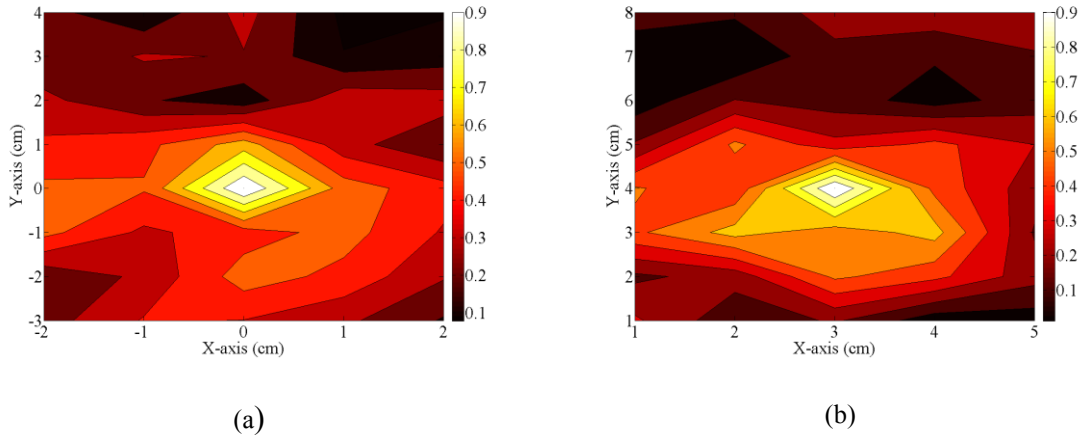


Figure 6 Imaging results of the back-propagated wave field $\mathbf{Y}_{IF}(\omega)$ for the same damage location with two different sensor positions. Figure (a) represents case 1 with the APC receiver transducer, whilst case 2 with the MFC sensor is shown in figure (b).

As illustrated in Fig. (6), the structural damage was detected in both cases with high level of accuracy. Hence the IF method in combination with PSA analysis was able to enhance the focusing efficiency with a grid spacing of 1 cm, even using one receiver transducer. Moreover, compared to other ultrasonic techniques for the imaging of the structural damage, this methodology not only needs a simple signal processing to locate the nonlinear source (with computational time less than 1 sec), but also it does not require any numerical routines to solve nonlinear system of equations, as well as a priori knowledge of the mechanical properties and the dispersion behaviour of the elastic GW. Future work is ongoing to extend this nonlinear imaging method to the detection and localisation of multiple damages.

V. CONCLUSIONS

Advanced composite materials are widely used in many sectors such as aerospace, marine, rail and automotive due to their high resistance to fatigue and corrosion, as well as their high strength to weight ratio. However, unlike metallic media, which are homogeneous and dissipate energy through yielding, composite structures are relatively brittle and exhibit weak interfacial strength between laminas. Indeed, due to their fragility to foreign object impacts, composite laminates present challenges for damage detection as much of the flaw is often interlaminar (e.g. sub-surface delamination, matrix cracking, fibre debonding or fracture, etc...) and not readily detectable. This paper presented an ultrasonic method for the detection of delamination in a composite structure showing primarily second order nonlinear elastic behaviour. Phase symmetry analysis, along with chirp excitation signal was used to characterise the second order nonlinearity of the

material by exploiting its invariant properties with the phase angle of the input waveforms. Then, a “virtual” inverse filtering imaging process, using only one receiver sensor, was used to “illuminate” the damaged zone. The robustness of this technique was experimentally demonstrated on a carbon fibre reinforced plastic panel undergone to impact loading. The results showed the effectiveness of this nonlinear imaging technique as it allowed achieving a perfect identification of the damage location.

References

- [1] F. Ciampa, M. Meo. “Impact localization on a composite tail rotor blade using an inverse filtering approach”. *Journal of Intelligent Material Systems and Structures*, **25** (15), pp. 1950-1958, (2014).
- [2] J.-B. Ih, F.-K. Chang. “Pitch-catch active sensing method in structural health monitoring for aircraft structures”. *Struct Health Monit* **7**(1), 5-19 (2008).
- [3] T. J. Ulrich, P. A. Johnson, R. A. Guyer. “Interaction dynamics of elastic waves with a complex nonlinear scatterer through the use of a time reversal mirror”. *Phys. Rev. Lett.* **98**, 104301/1-4 (2007).
- [4] R. A. Guyer, P. A. Johnson. “Nonlinear mesoscopic elasticity: evidence for a new class of materials”. *Phys Today* **52**, 30-36 (1999).
- [5] M. Meo, G. Zumpano. “Nonlinear elastic wave spectroscopy identification of impact damage on sandwich plate”. *Compos Struct* **71**, 469–474 (2005).
- [6] K. E.-A. Van Den Abeele, P.-A. Johnston, A. Sutin. “Nonlinear elastic wave spectroscopy (NEWS) techniques to discern material damage, part I: nonlinear wave modulation spectroscopy (NWMS)”. *Res. Nondestr. Eval.* **12** (1), 17-30 (2000).

- [7] F. Ciampa, S. Pickering, G. Scarselli, M. Meo, “Nonlinear damage detection in composite structures using bispectral analysis”, *Proc. SPIE. 9064, Health Monitoring of Structural and Biological Systems 2014*, doi: 10.1117/12.2046631, San Diego, (2014).
- [8] M. Scalerandi, A. S. Gliozzi, C. L. E. Bruno, D. Masera and P. Bocca, “A scaling method to enhance detection of a nonlinear elastic response”, *Appl. Phys. Lett.* **92** 101912, (2008).
- [9] S. Dos Santos, Z. Prevorovsky. “Imaging of human tooth using ultrasound based chirp-coded nonlinear time reversal acoustics”. *Ultrasonics*, **51**, 667-674 (2011).
- [10] F. Ciampa, M. Meo, “Nonlinear elastic imaging using reciprocal time reversal and third order symmetry analysis”, *J. Acoust. Soc. Am.* **131**, pp. 4316–4323 (2012).
- [11] L.-D. Landau, E.-M. Lifshitz, *Theory of Elasticity*, Chap. III, Pergamon, Oxford, (1986).
- [12] F. Ciampa, E. Barbieri, M. Meo, “Modelling of multiscale nonlinear interaction of elastic waves with three dimensional cracks”, *J. Acoust. Soc. Am.* **135** (4), (doi: 10.1121/1.4868476), (2014).
- [13] F. Ciampa, E. Onder, E. Barbieri, M. Meo, “Detection and Modelling on Nonlinear Elastic Response in Damaged Composite Structures”, *J Nondestruct Eval*, (doi: 10.1007/s10921-014-0247-7), (2014).
- [14] O. Bou Matar, P.-Y Guerder, Y. Li, B. Vandewoestyne, K. E.-A. Van Den Abele. “A nodal discontinuous Galerkin finite element method for nonlinear elastic wave propagation”. *J. Acoust. Soc. Am.* **131** (5), pp. 3650-63 (2012).
- [15] E. Barbieri, M. Meo. “Time reversal DORT method applied to nonlinear elastic wave scattering”. *Wave Motion* **47** (7), 452–467 (2010).

- [16] P. Delsanto, M. Scalerandi, “A spring model for the simulation of the propagation of ultrasonic pulses through imperfect contact interfaces”, *J. Acoust. Soc. Am.*, **104**, 2584 (1998).
- [17] T. Goursolle, S. Callè, S. Dos Santos, O. Bou Matar. “A two dimensional pseudospectral model for time reversal (TR) and nonlinear elastic wave spectroscopy (NEWS)”. *J. Acoust. Soc. Am.* **122** (6), 3220–3229 (2007).
- [18] C. Pecorari. “Adhesion and nonlinear scattering by rough surfaces in contact: Beyond the phenomenology of the Preisach-Mayergoyz framework”, *J. Acoust. Soc. Am.*, **116**, pp. 1938–47 (2004).
- [19] I.-Y. Solodov, “Ultrasonics of Non-Linear Contacts: Propagation, Reflection and NDE-Applications”, *Ultrasonics*, **36**, pp. 383–390, (1998).
- [20] T. J. Ulrich, A. M. Sutin, T. Claytor, P. Papin, P. Y. Le Bas, J. A. TenCate. “The time reversed elastic nonlinearity diagnostic applied to evaluation of diffusion bonds”. *Appl. Phys. Lett.* **93**, 151914 (2008).
- [21] F. Ciampa, S. Pickering, G. Scarselli, A. Gianpiccolo, M. Meo, “Nonlinear Elastic Tomography using Sparse Array Measurements”, In: *Proc. of EWSHM - 7th European Workshop on Structural Health Monitoring, Jul 2014, Nantes, France*, <hal-01022040> (2014).
- [22] B.E. Anderson, M. Griffa, T.J. Ulrich, P.A. Johnson, “Time reversal reconstruction of finite sized sources in elastic media”, *J. Acoust. Soc. Am.*, **130**, pp. EL219–EL225, (2011).
- [23] C. Prada, S. Manneville, D. Spoliansky, M. Fink “Decomposition of the time reversal operator: detection and selective focusing on two scatterers”. *J. Acoust. Soc. Amer.* **99**, 2067–2076 (1996).

- [24] M. Frazier, B. Taddese, T. Antonsen, and S. M. Anlage, “Nonlinear time reversal in a wave chaotic system”, *Phys. Rev. Lett.* **110**, 063902, (2013).
- [25] X.S. Guo, D. Zhang, J. Zhang, “Detection of fatigue-induced micro-cracks in a pipe by using time-reversed nonlinear guided waves: a three-dimensional model study”, *Ultrasonics* **52** (7), pp. 912–919, (2012).
- [26] M. Fink. “Time reversal of ultrasonic fields. I: Basic principles”, *IEEE Trans. Ultrason. Ferroelec. Freq. Contr.* **39** (5), 555–566 (1992).
- [27] M. Tanter, J. L. Thomas, M. Fink. “Focusing and steering through absorbing and aberrating layers: Application to ultrasonic propagation through the skull”. *J. Acoust. Soc. Am.* **103** (5), 2403–10 (1998).
- [28] Quieffin N. “Etude du rayonnement acoustique de structures solides: vers un systeme d' imagerie haute resolution”. PhD thesis, University Paris VI (2004).
- [29] S. Dos Santos, S. Vejvodova, Z. Prevorovsky. “Nonlinear signal processing for ultrasonic imaging of material complexity”, in: Proc. Estonian Academy of Sciences, **59**, 301-311 (2011).
- [30] T. Misaridis, J A. Jensen. “Use of modulated excitation signals in medical ultrasound. Part II. Design and Performance for Medical Imaging Applications”. *IEEE Trans. Ultrason, Ferroelect, Freq. Contr.* **52** (2), 192-207 (2005).
- [31] T. Misaridis, J A. Jensen. “Use of modulated excitation signals in medical ultrasound. Part II. Design and Performance for Medical Imaging Applications”. *IEEE Trans. Ultrason, Ferroelect, Freq. Contr.* **52** (2), 192-207 (2005).
- [32] W. Greblicki. “Nonparametric approach to Wiener system identification”. *IEEE Trans. Circ. Syst. - I: Fundamental Theory and Applications* **44** (6), 538–545 (1997).